Proposal of a Diamond-based Beam Halo Monitor for an Energy Recovery Linac

Hideki Aoyagi, T. Bizen , T. Itoga, N. Nariyama
JASRI / SPring-8

Y. Asano, T. Tanaka, H. Kitamura
RIKEN/ SPring-8

OUTLINES

1. Introduction
   Purpose of the halo monitor, Required detection limit
   Principle verification tests of diamond detector
2. Feasibility tests using a prototype of the halo monitor
3. Adoption of RF fingers to the halo monitor
4. Operational Experience at SACLA
5. Summary

SACLA

SPring-8 Angstrom Compact Free Electron Laser

H. Tanaka, IPAC2011 Invited talk, MOYCA01

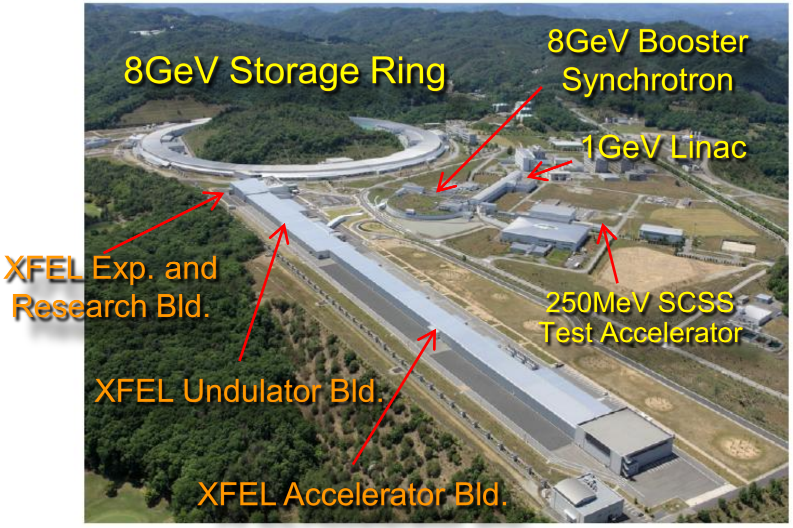

Figure 1: Aerial photo of SACLA.

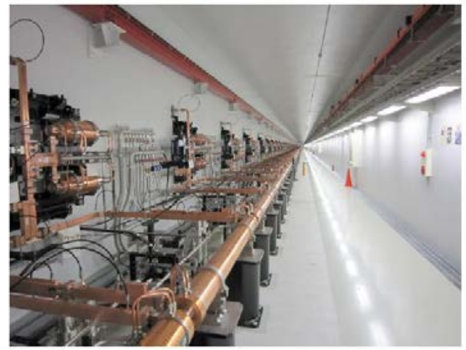

Figure 5: C-band acceleration system in the tunnel.

Figure 3: Picture of the SACLA injector section.

Table 1 Main Design Parameters

Parameter	Target Value
Beam energy (GeV)	4~8
Bunch compression ratio	> 3000
Peak current (kA)	3~4
Repetition rate (Hz)	Max. 60
Normalized slice emittance (π μmrad)	< 1
Shortest SASE laser wavelength (Angstrom)	0.6
Laser power (GW)	20~30
K-value setting range	1.1~2.2
Undulator period length (mm)	18
Number of undulator periods	277
Number of undulator segments	18

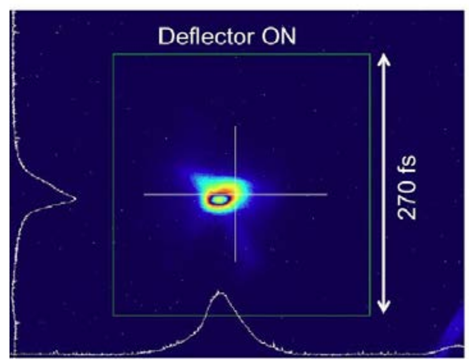

Figure 7: Vertically streaked profile of the fully compressed bunch.

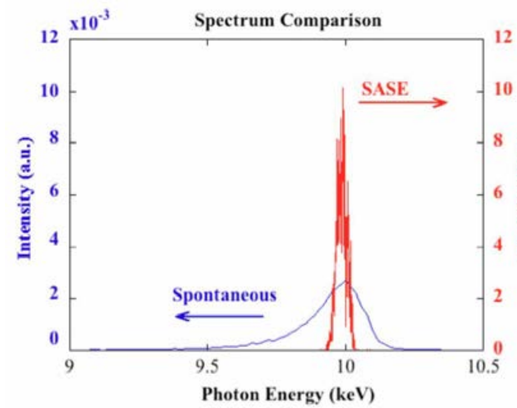

Figure 8: SASE laser spectrum at 10 keV.

Purpose of the Halo Monitor

In order to protect the undulator permanent magnets against radiation damage, Beam Halo Monitor has been installed in front of the in-vacuum undulators.

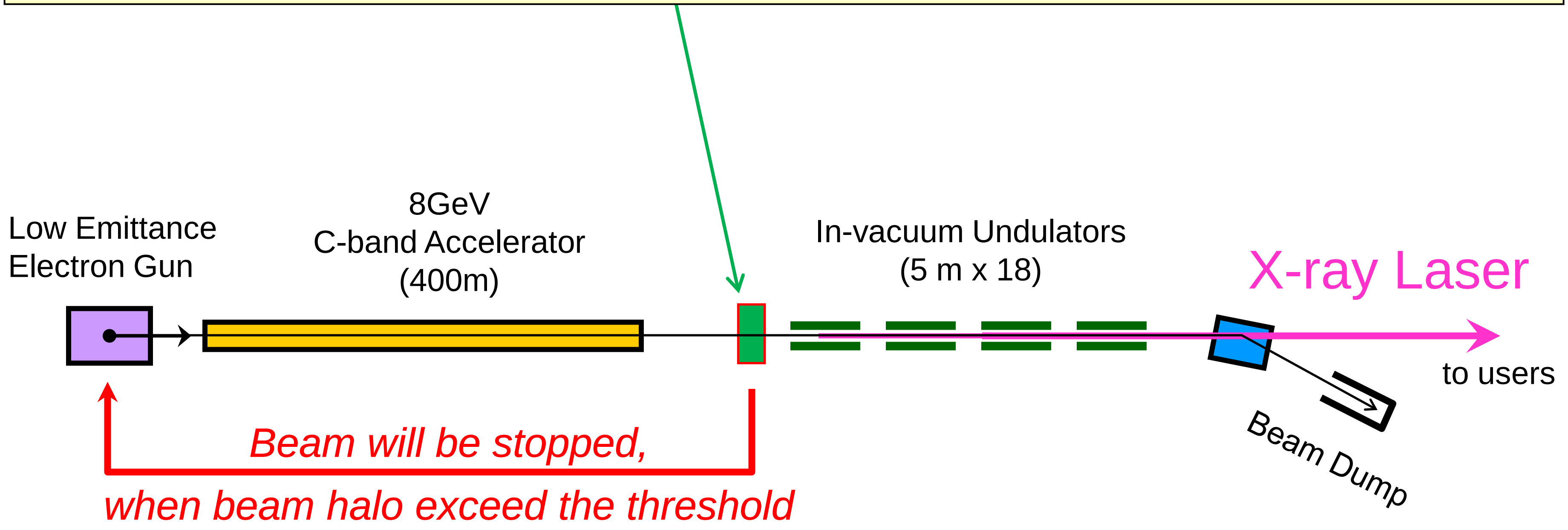

Schematic layout of SACLA

Required Detection Limit

Tolerance of demagnetization rate of undulator magnets

1 % / 10 year

→ Tolerance of incident electron on the magnets

4×10^{14} e^- / 10 year (based on the experimental results)

→ Required detection limit $< 2 \times 10^{4}$ e^- / pulse

(60Hz × 24hrs × 365day × 10 year ⇒ 1.9×10^{10} pulse)

→ Tolerance of electron loss rate $< 10^{-5}$

cf. Number of electron through undulators

2×10^{9} e^- / pulse (0.3nC/pulse)

How to measure?

Ideally

Measure a differential of charge between before and after undulators.

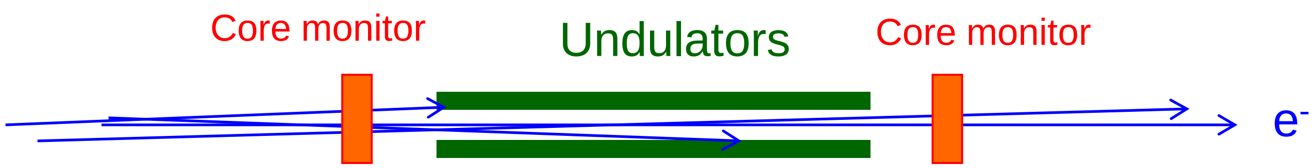

Required resolution must be less than 10^{-6}.

Realistically

Measure a beam halo in front of undulator permanent magnets.

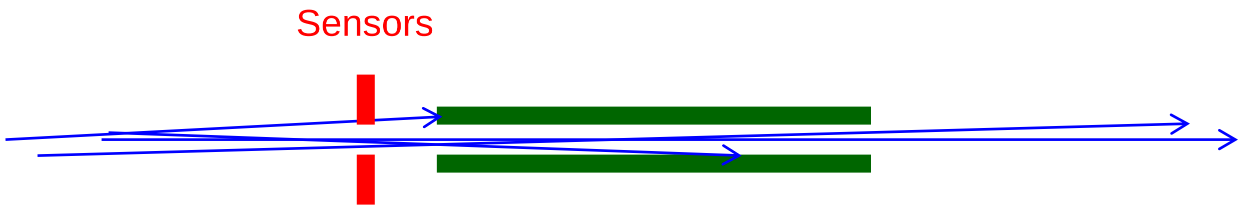

Direct measurement in the beam duct

We adopted this type.

Configuration of sensors ?

A single large detector with a hole in center.

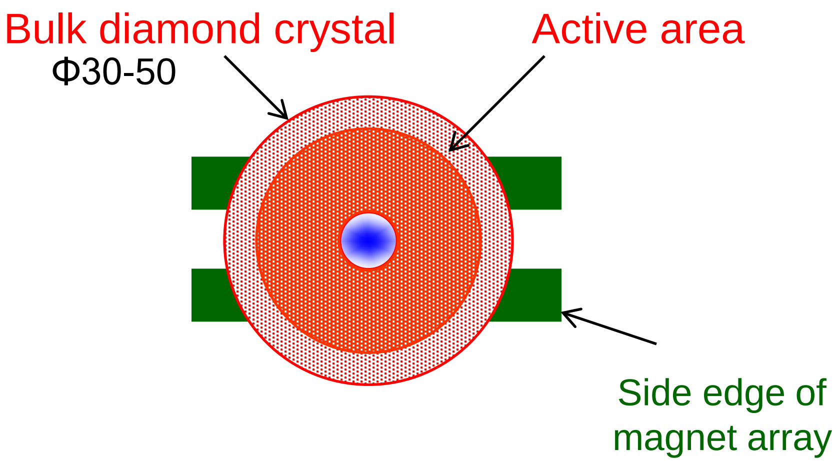

- ○ Wide active area
- × Fixed aperture
- △ Longer time constant, $\tau = RC$

A pair of detectors with separate actuators

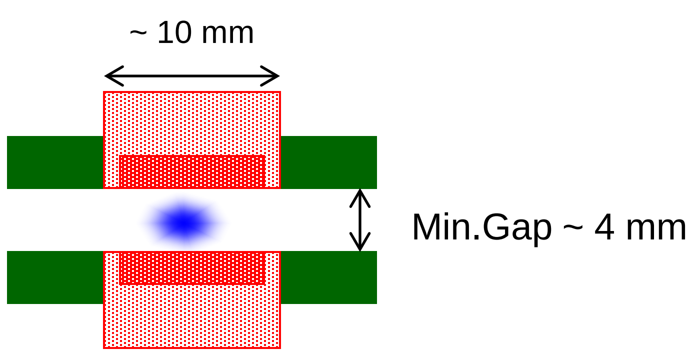

- △ Small active area
- ◎ Variable aperture
- ○ Short time constant
- ○ Easy to fabricate (small crystal)

We adopted the this type.

Diamond detector as semi-conductor detector

e-h pairs are generated in the bulk of diamond crystal.

Beam core passes through between diamond detectors.

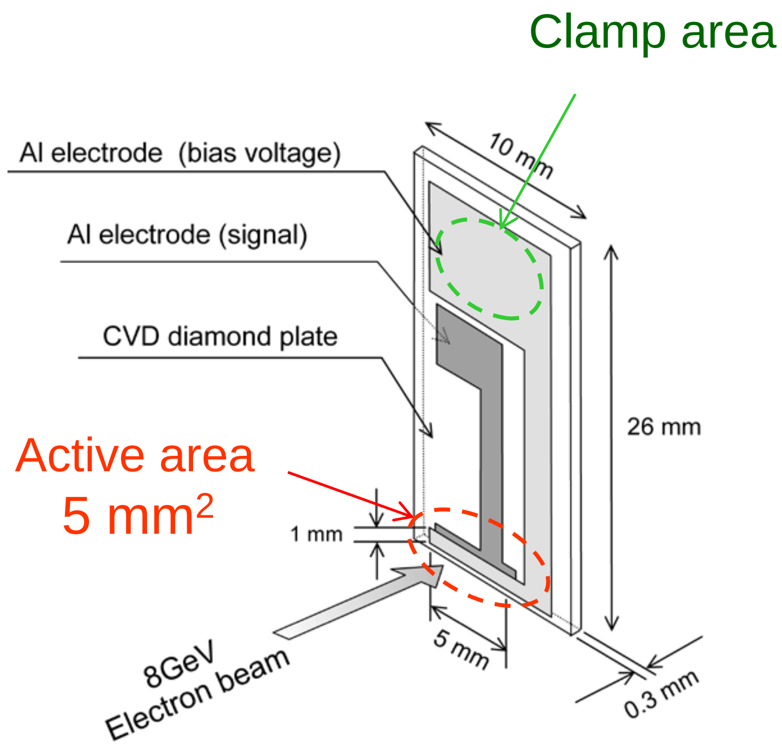

Manufactured by Kobelco

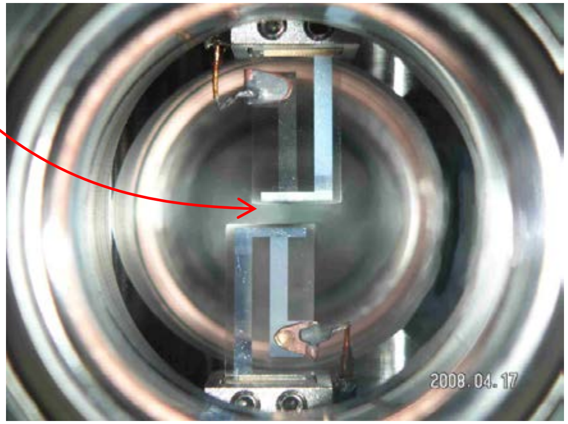

Seen from on the axis

Advantages of diamond :

- High radiation hardness (durable)
- Good heat resistance (bakable)
- High insulation resistance (low dark current)

Principle verification tests of diamond detector

Carried out at 8GeV booster synchrotron

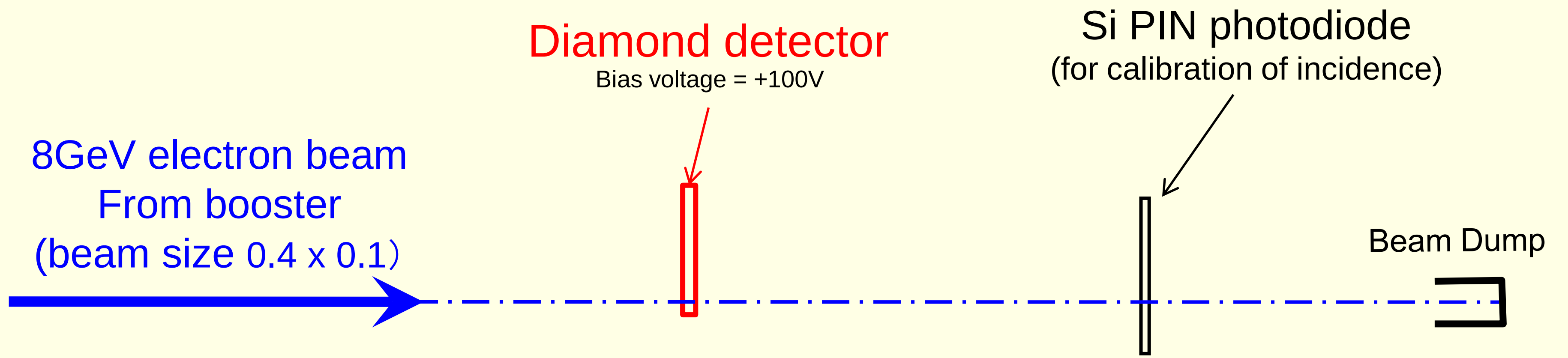

Check of pulse shape

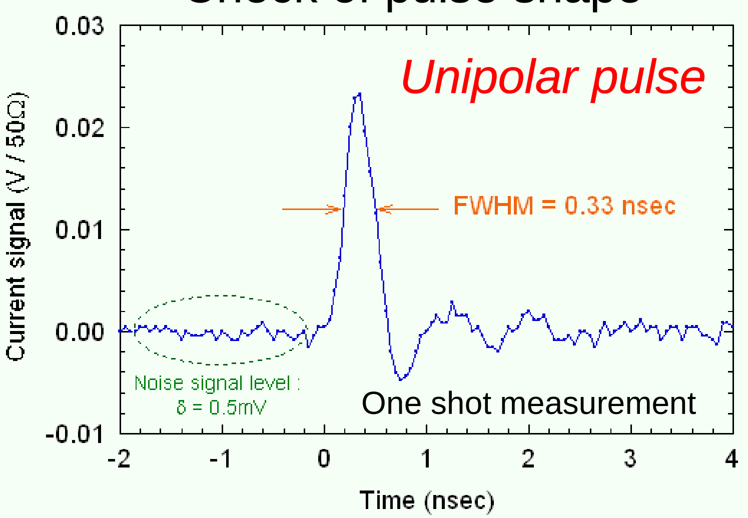

Linearity check

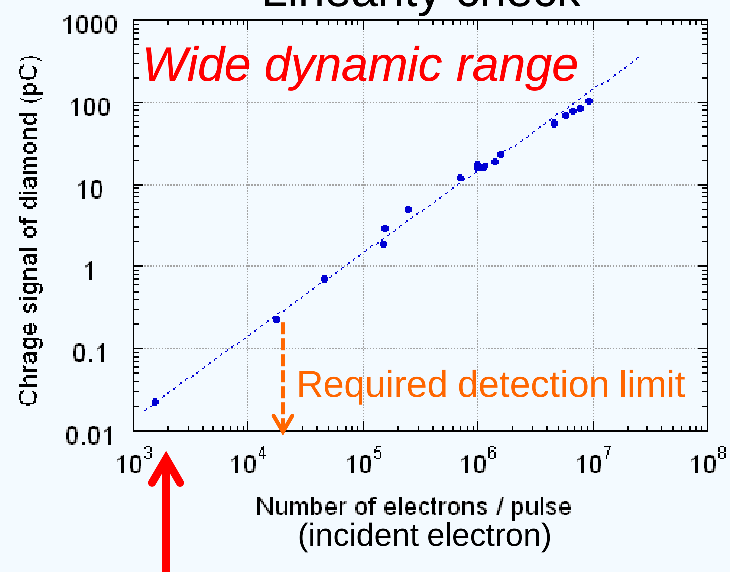

Practical detection limit is 2×10^3 e^- /pulse.

Definition : 10σ of noise signal level

2. Photographs of the Prototype

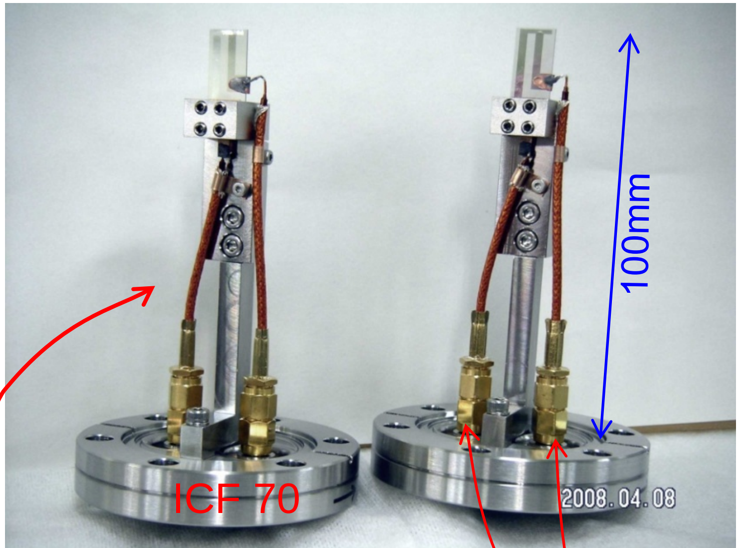

Kapton coaxial cable

SMA connectors

Installed at 250MeV SCSS Test Accelerator

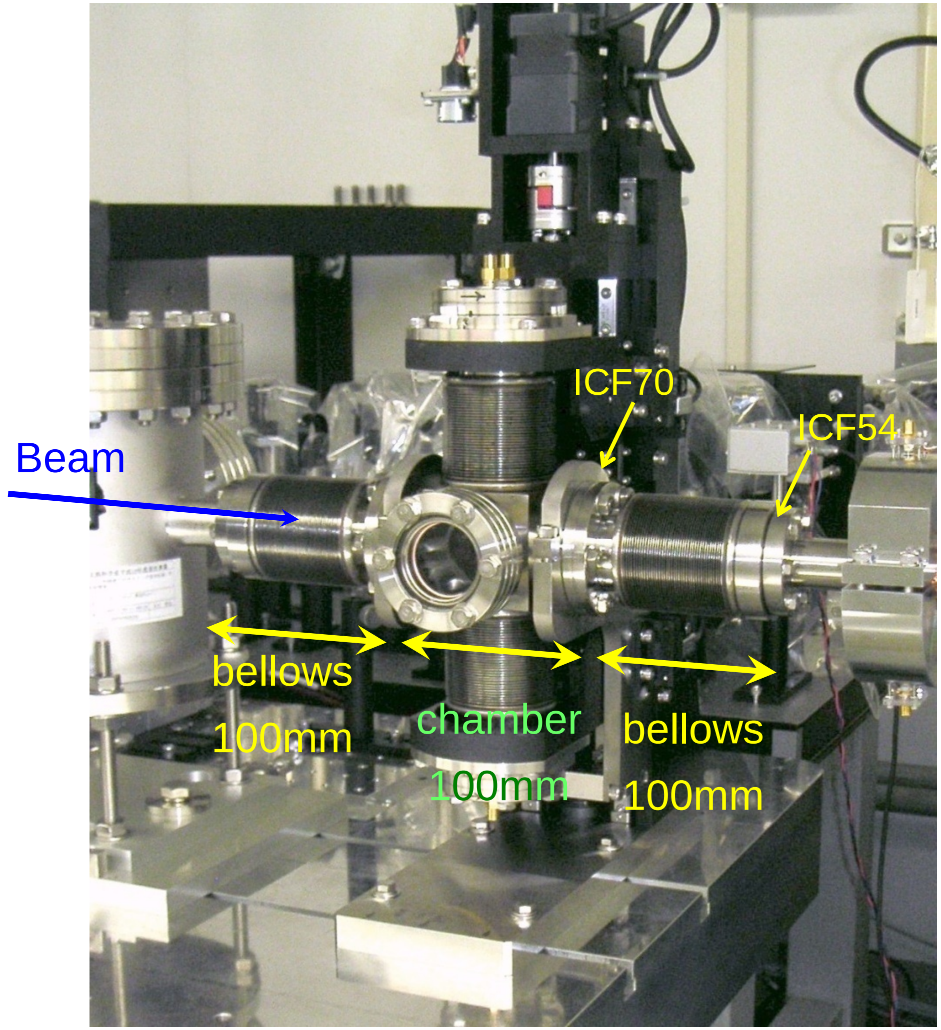

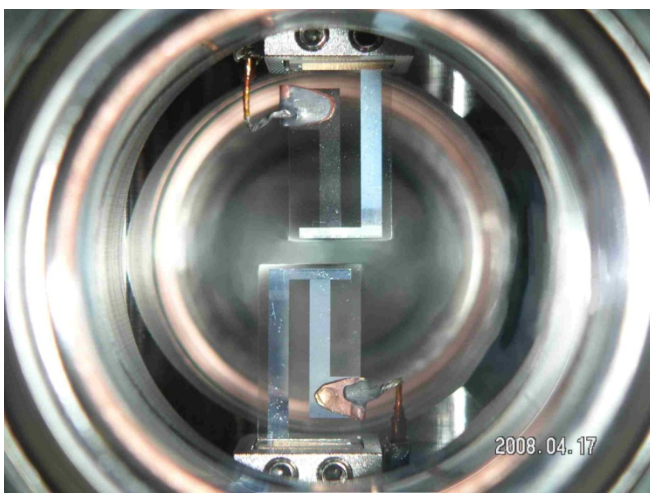

Seen from on the axis

Effect of Wake Field and their suppression

Measured at SCSS Test Accelerator

The active area of the diamond detector was irradiated directly with weak beam core (3×10^4 e).

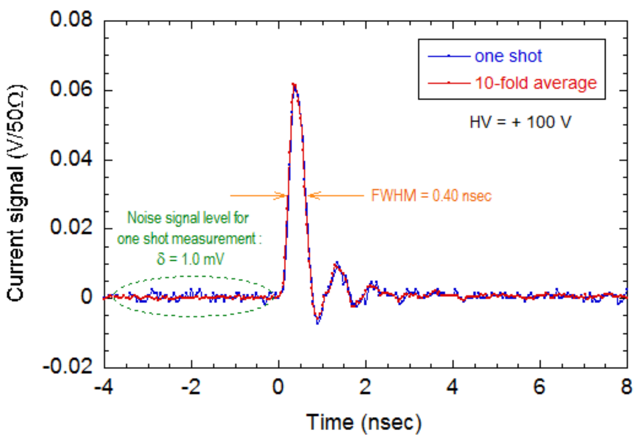

The unipolar pulse shape can be observed clearly.

The strong beam core passes through near the edge of diamond detectors.

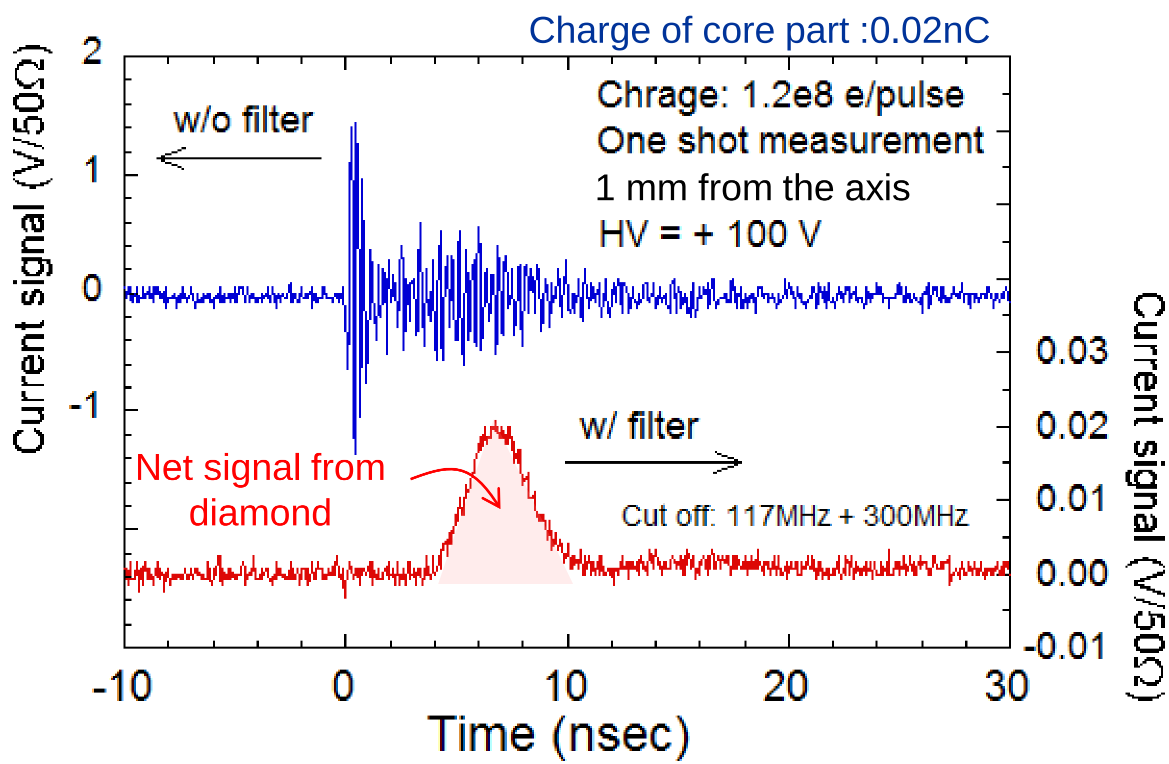

The effect of induction current can be smeared by using Low Pass Filters, so the net signal from e-h pairs that is created by the halo part of the electron beam can be measured.

Profile measurement of the beam halo

Measured at SCSS Test Accelerator

Scanning in the vertical direction

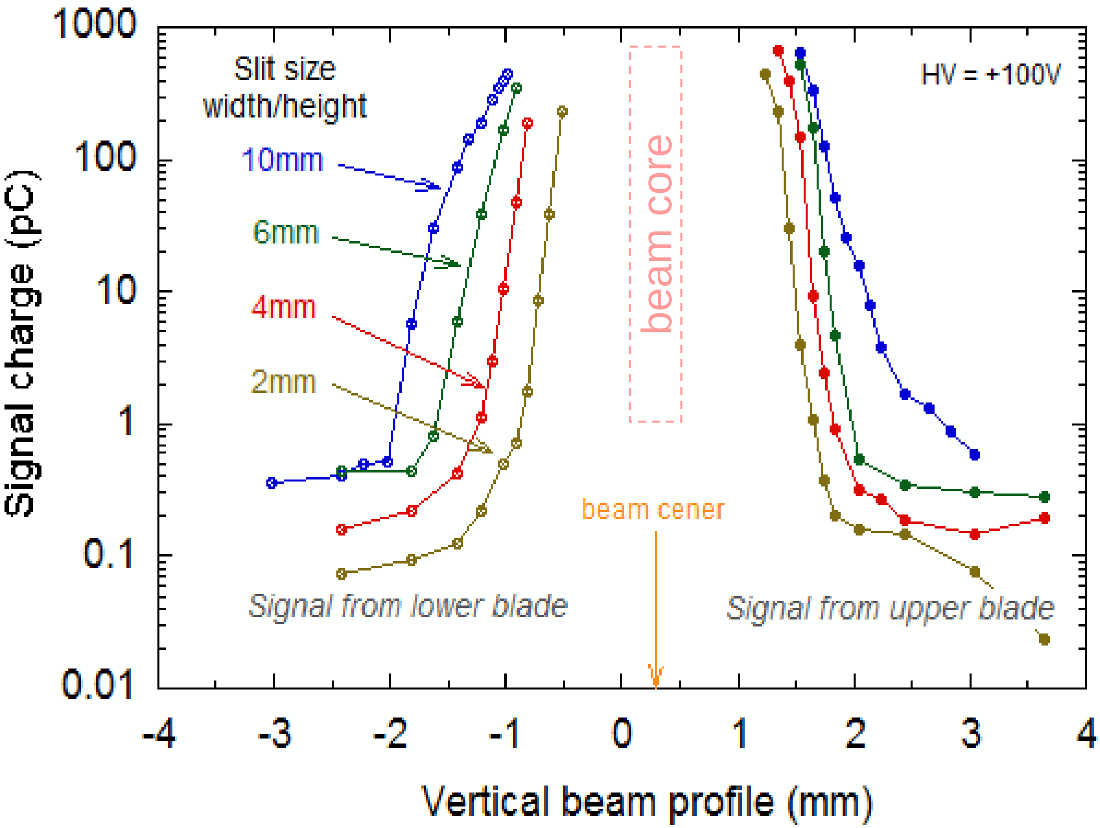

Slit width =

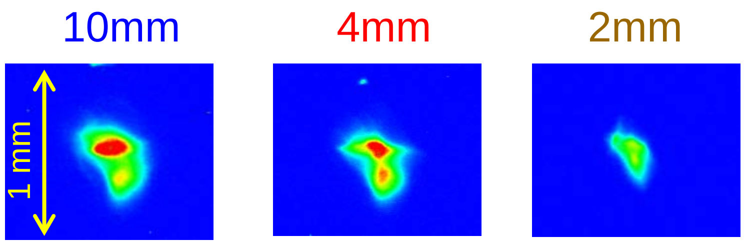

Images of OTR screen just after beam halo monitor

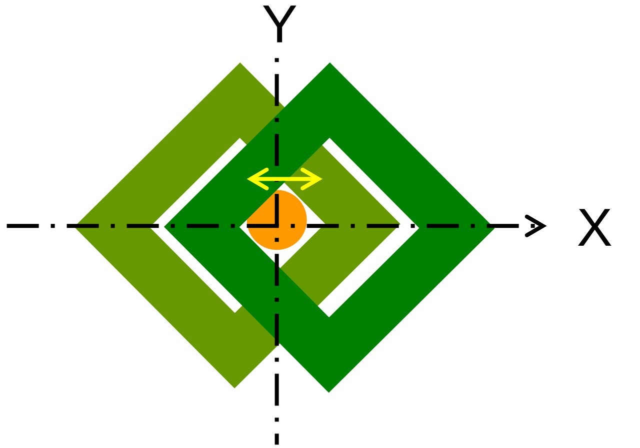

Spatial slit after 50 MeV Injector

Stability Tests of the Halo Monitor at the SCSS

IPAC2010, WEPEB068

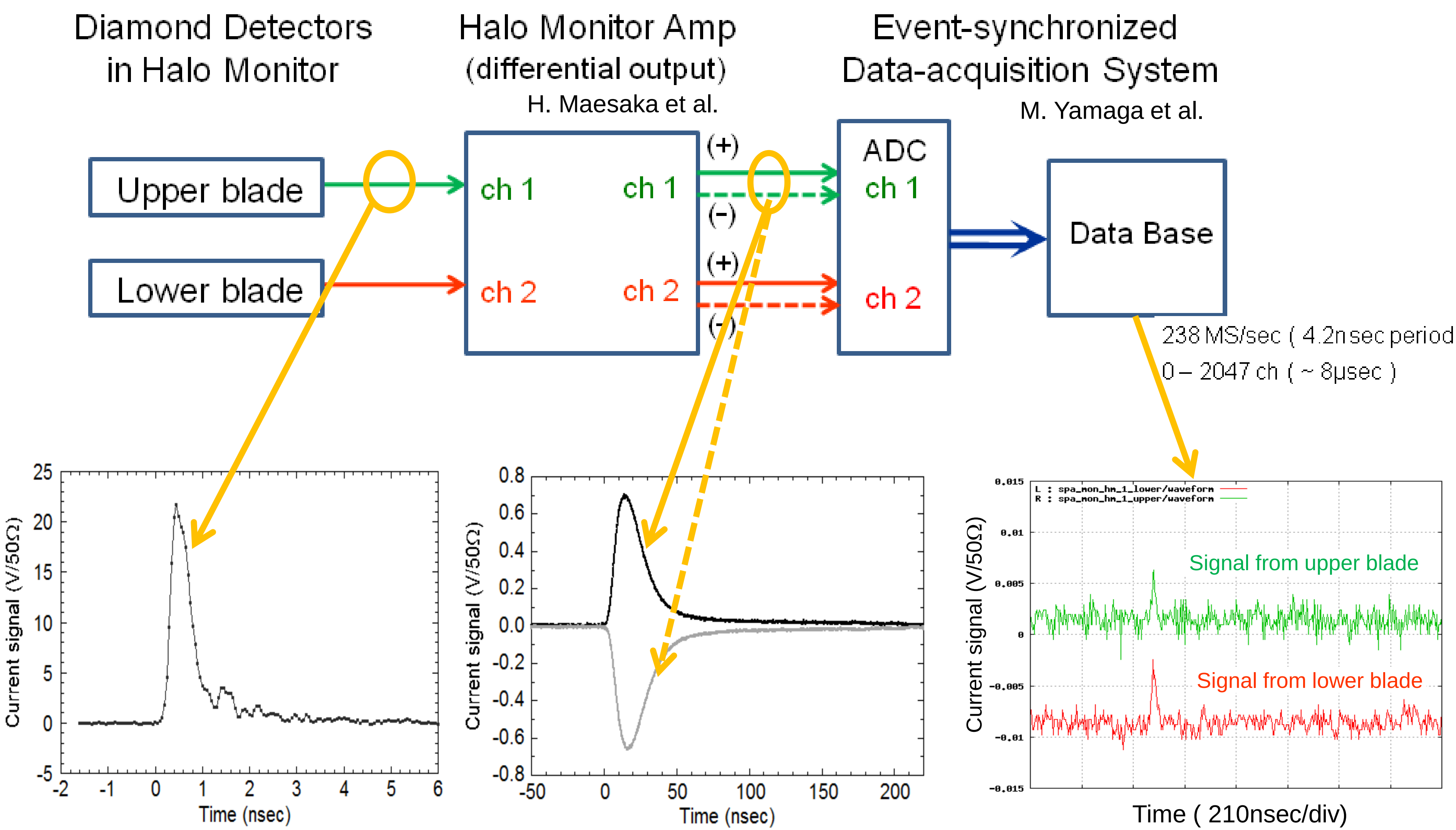

(a) The output signal from the diamond detector

(b) The output signal from the pre-amplifier.

(C) The waveform stored at data base.

Result of stability tests *in one day*

Measured at SCSS Test Accelerator

during machine study

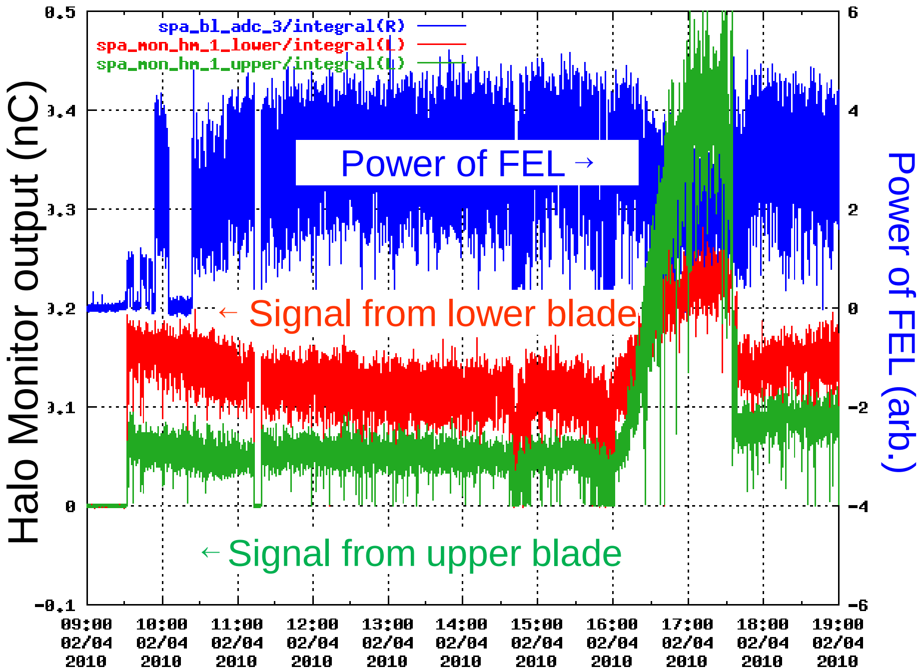

9am 7pm

during user operation

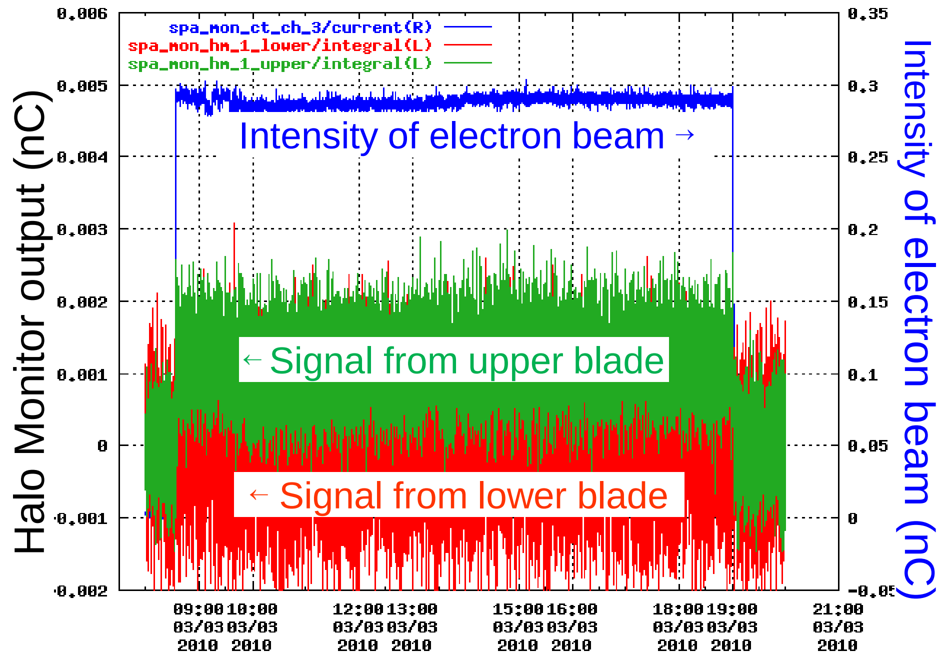

9am 7pm

3. Adoption of RF Fingers

FEL2010, THOC4
DIPAC2011, MOOB03

Finger type 0 (no fingers)	Finger type 1 (not covered)	Finger type 2 (fully covered)

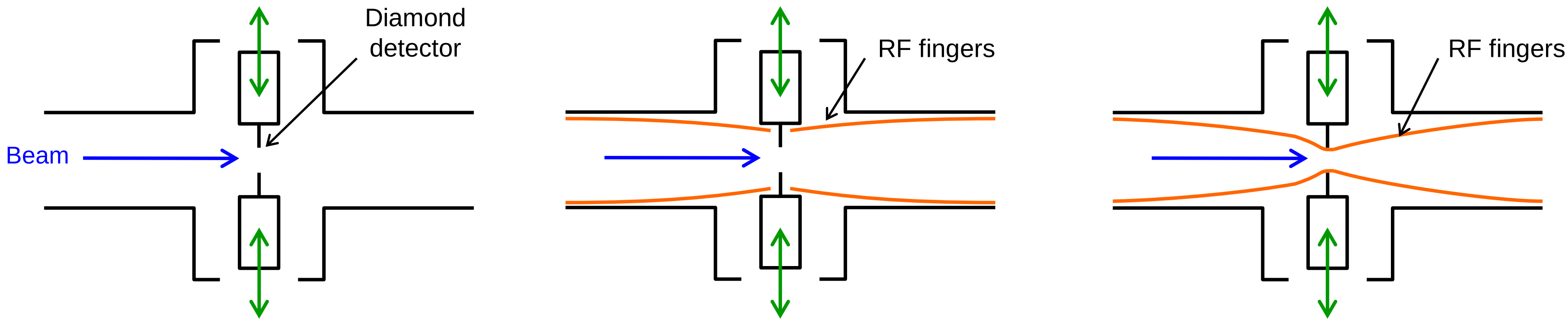

In the configuration of type 1, the active areas of the diamond detectors project from between RF fingers.

In the configuration of type 2, the RF fingers are connected without bumps.

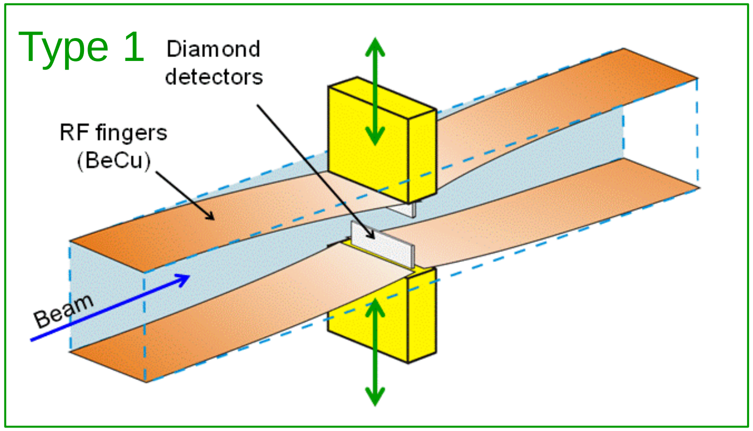

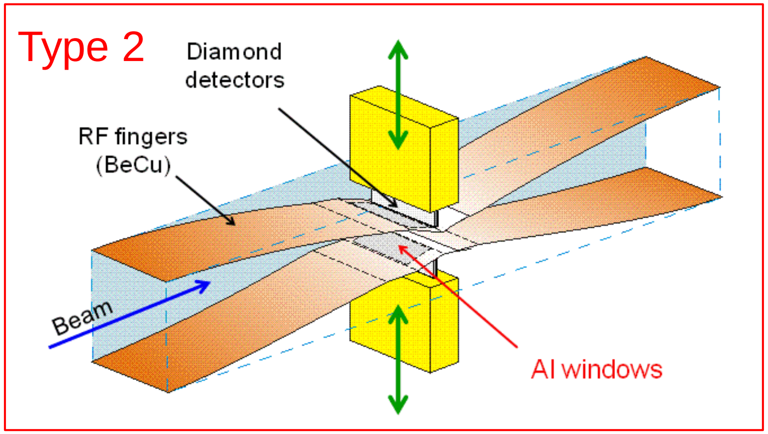

→ *We need to know,*
if the fingers can reduce induced current, and
if the signal blows up by radiation from the finger material.

Reduction of induced current *at SCSS Test Accelerator*

FEL2010, THOC4
DIPAC2011, MOOB03

Finger type 0
(no fingers)

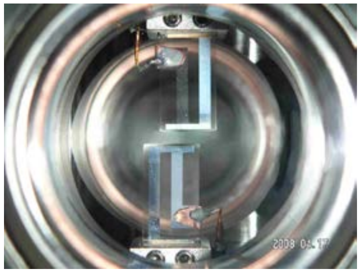

Finger type 1
(not covered)

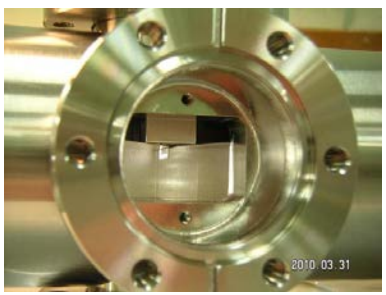

Finger type 2
(fully covered)

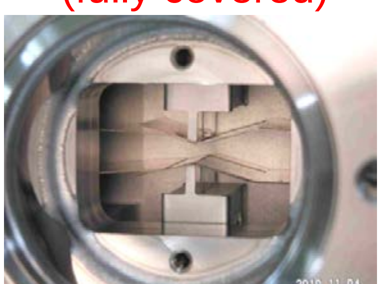

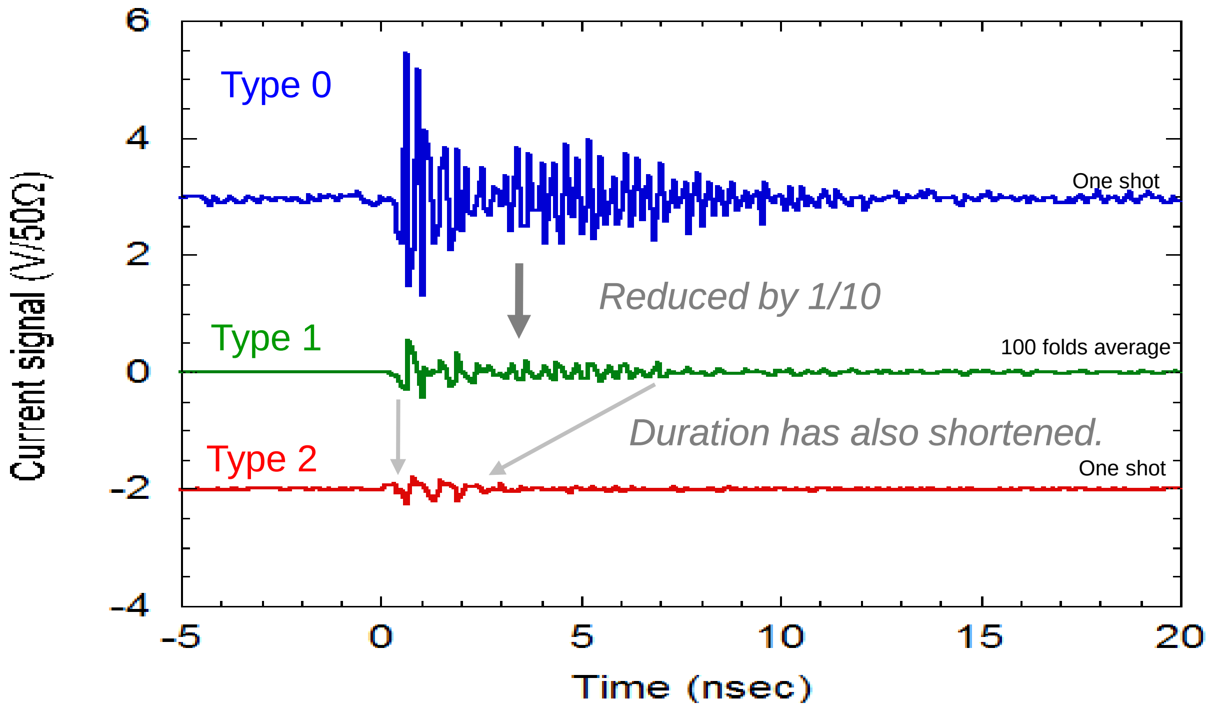

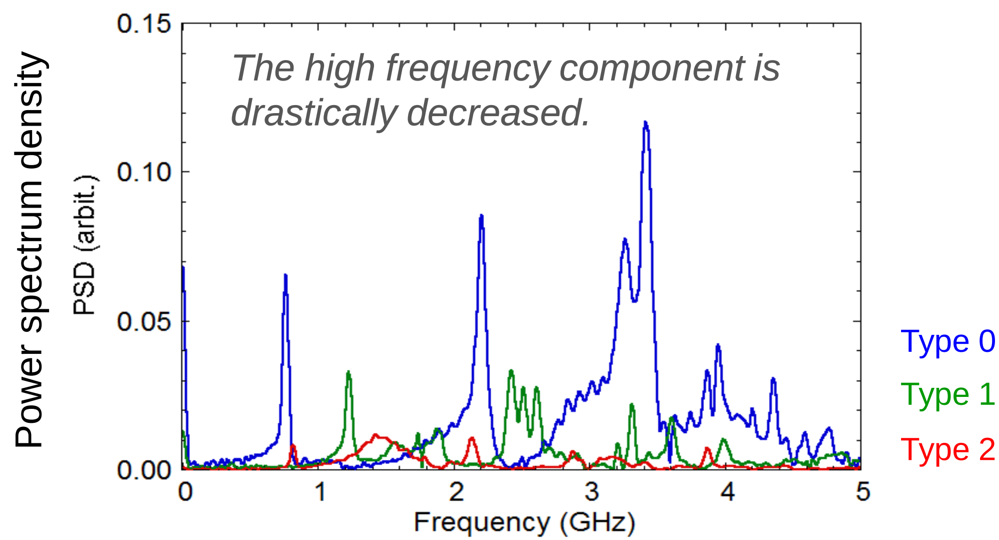

Radiation from RF fingers: experimental setup

DIPAC2011, MOOB03

Purpose of this measurement is to evaluate a variation of the detective efficiency caused by secondary electrons and bremsstrahlung that are generated in the finger material.

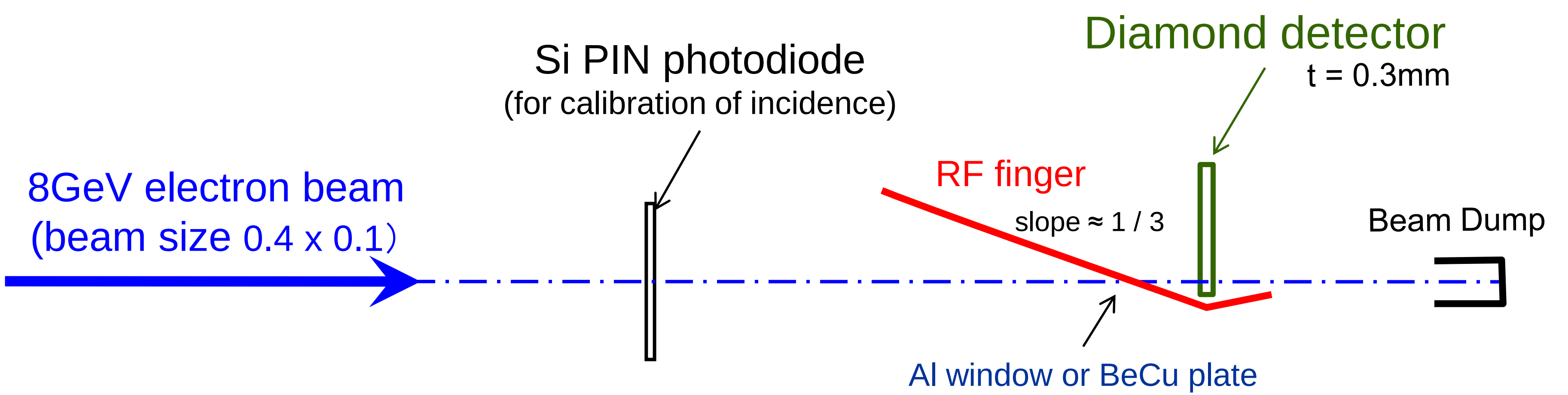

Carried out at 8GeV booster synchrotron

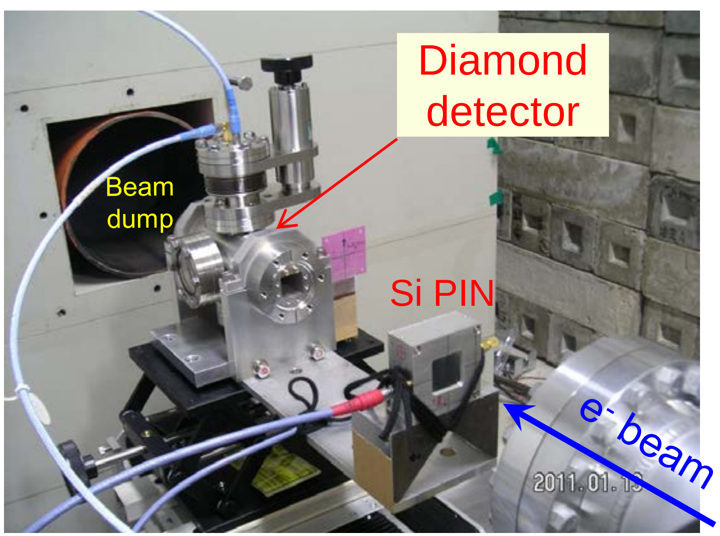

Experimental conditions

Finger type	Material	Thickness	Pass length
no finger	**none**	0 mm	**0 mm**
Al window	**Al**	0.1mm	**0.3mm**
BeCu x 1	**BeCu**	0.2mm	**0.6mm**
BeCu x 3	**BeCu**	0.6mm	**1.8mm**

experimental results and simulation results

Measurement data were normalized as the measurement value with no fingers is corresponding to the energy deposition of 0.16MeV/e, which is the simulation result at thickness = 0.

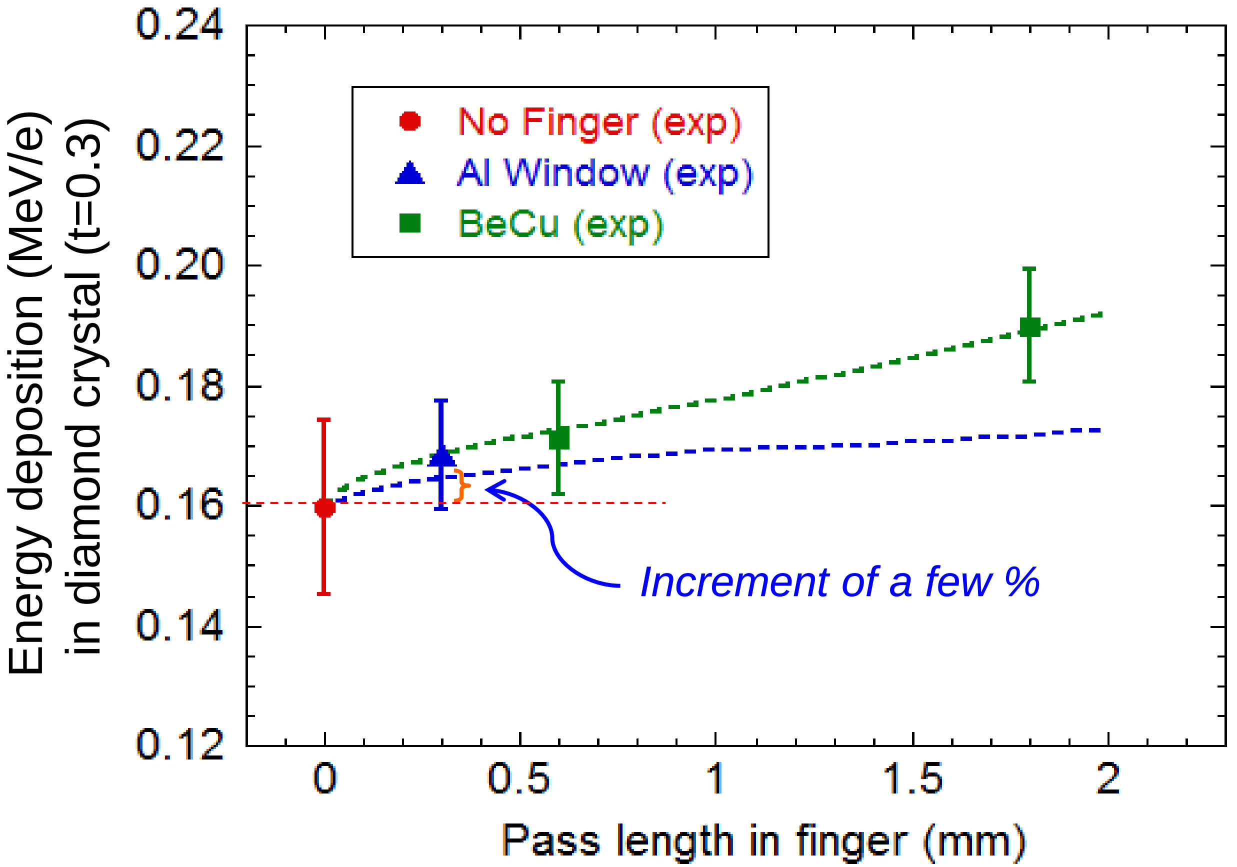

Monte Carlo simulation code:

EGS5

The experimental results and the simulation results are in good agreement within the measurement errors.

RF finger with Al window can be used for our purpose.

4. Installation at *SACLA*

IPAC2011, TUPC091

T. Hara et al.

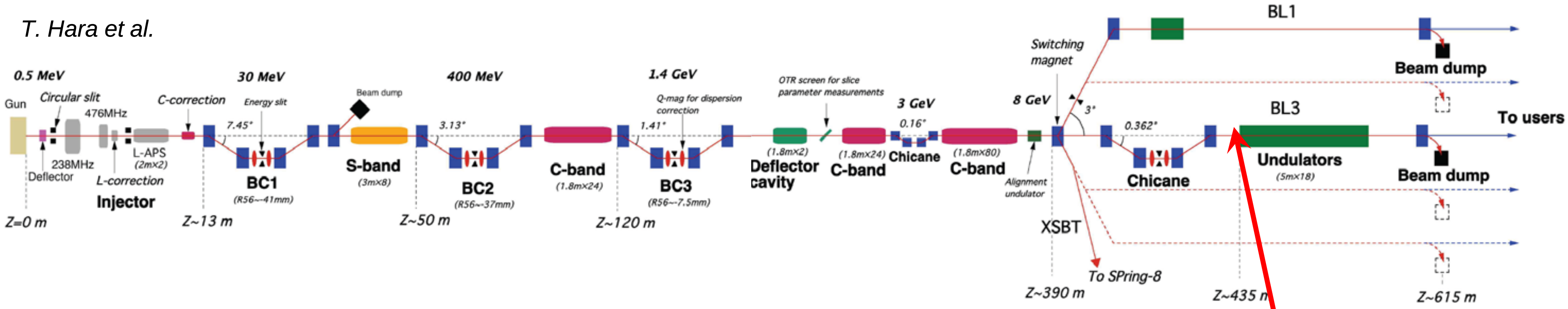

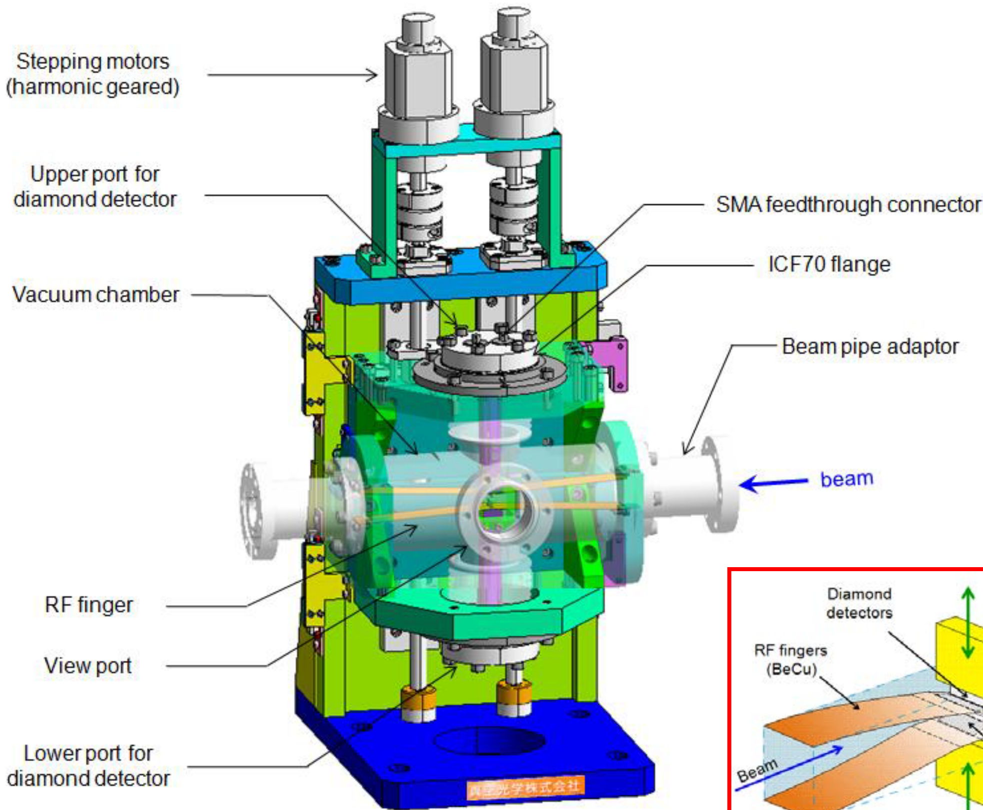

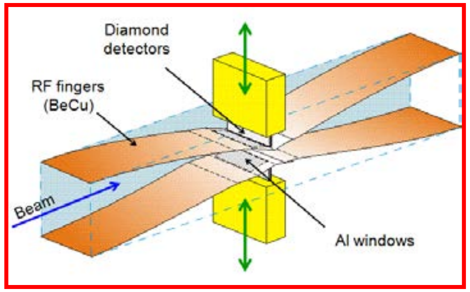

The geomagnetic shield box(blue box) is for beam based alignment.

Suppression of residual induced current

IPAC2011, TUPC091

Measured at SACLA

without Low Pass Filter

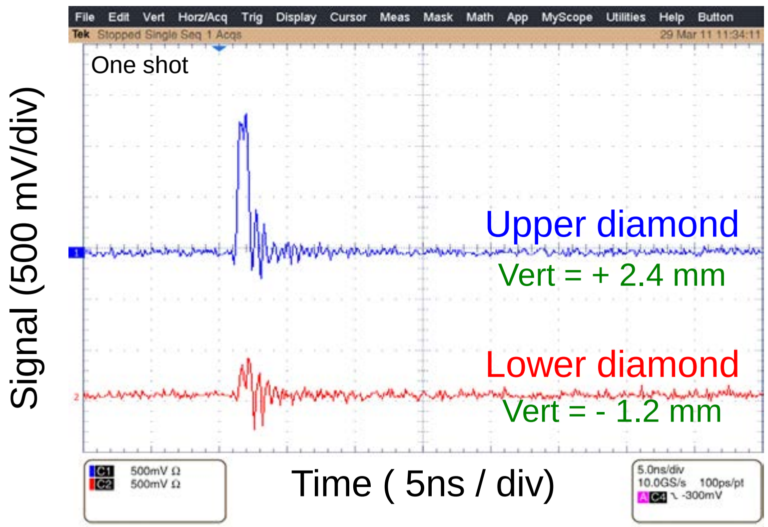

with Low Pass Filter

fc = 117 MHz & 300 MHz

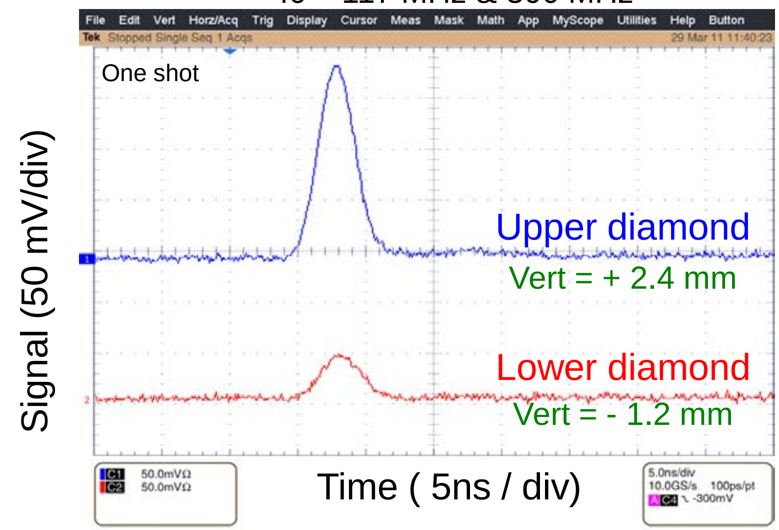

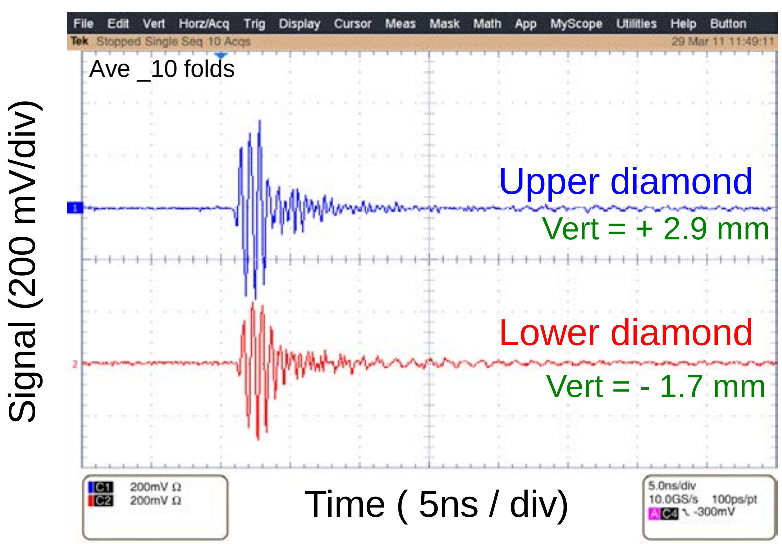

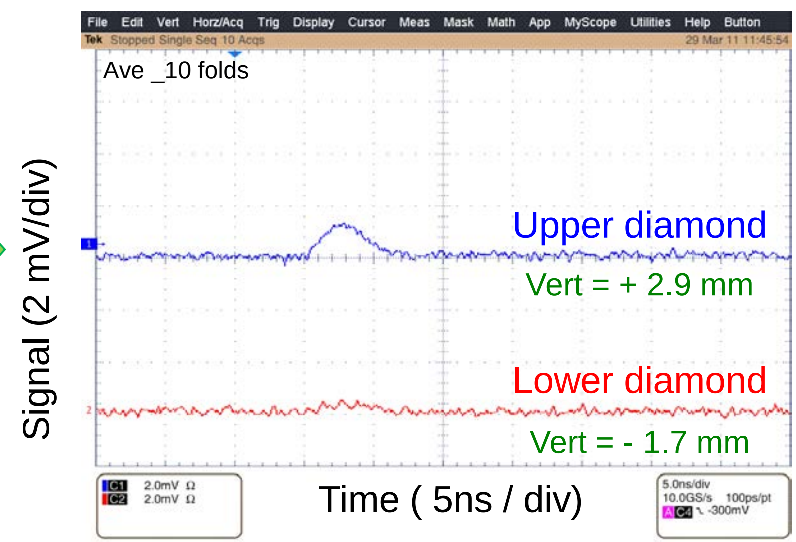

Trend graph of laser power while RF fingers are closed

Measured at SACLA

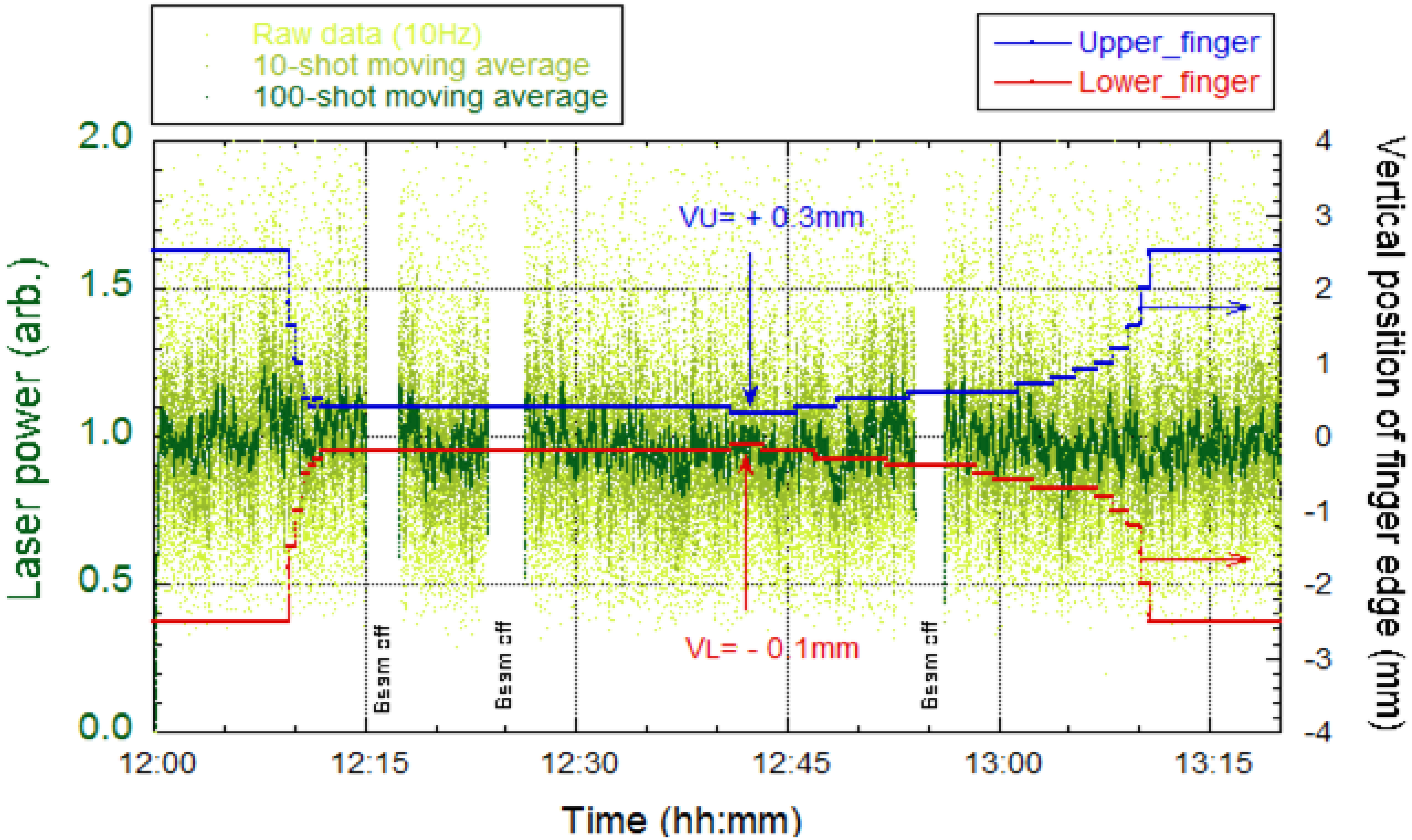

The laser power did not received a significant change even at the minimum gap.

We conclude that this is an effect of reducing the wake field by the RF fingers.

Profile measurement of the beam halo

IPAC2011, TUPC091

Measured at SACLA

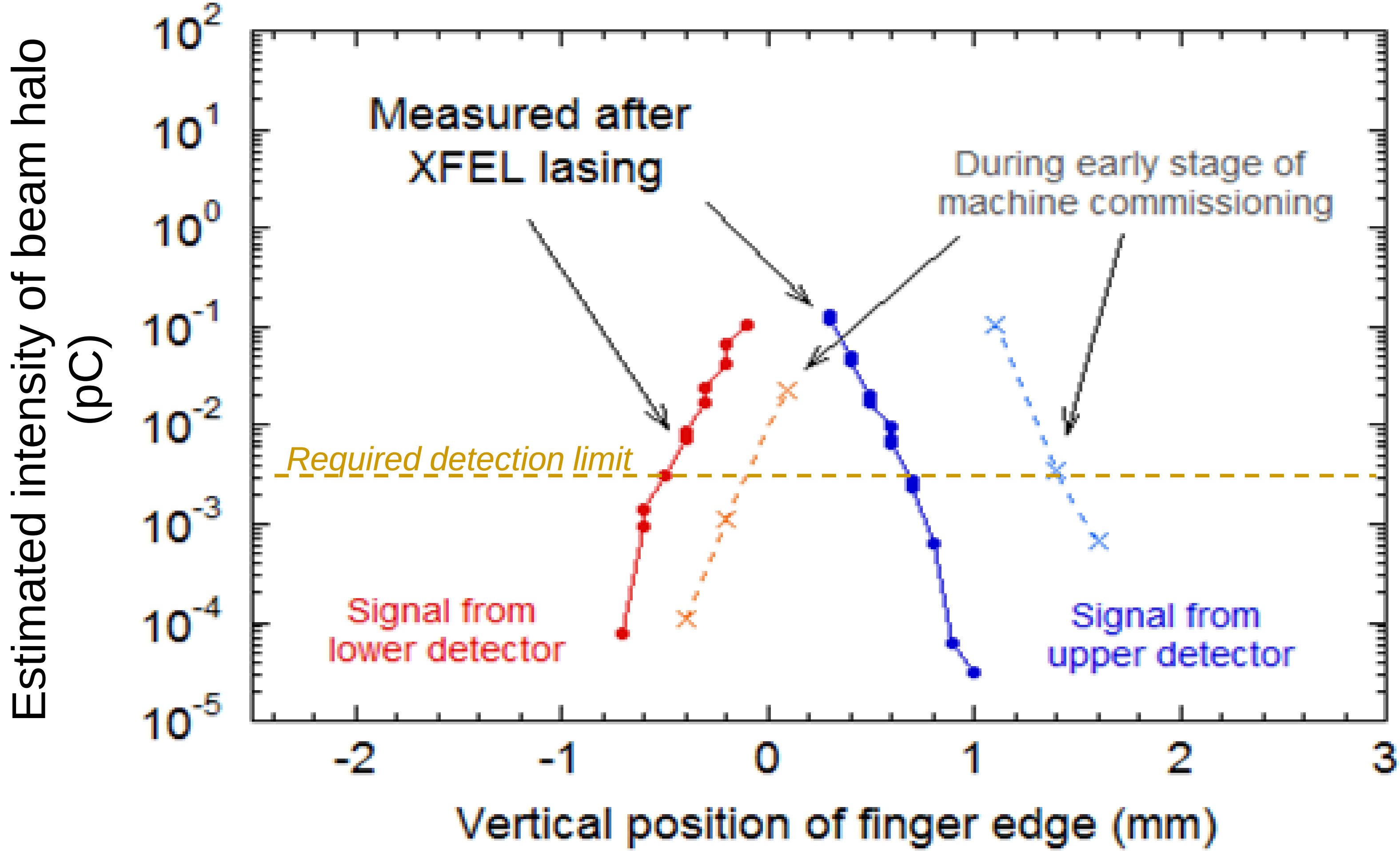

We succeeded in achieving the required detection limit at SACLA.

Notice: When the edge of the RF finger is near the beam core, the output signals of diamond detectors blow up because of scattering.

5. Summary

1. Purpose of this work

- to protect undulator magnets against radiation damage
- using the beam halo monitor equipped with the diamond detectors
- adopting pulse measurement for enhancing S/N ratio

2. Performances of the Halo Monitor

- Practical detection limit is about 2×10^3 e/pulse. (1ppm of 0.3nC)
- Dynamic range is 4 orders. (2×10^3 to 10^7 e/pulse)
- Feasibility had been demonstrated.
- RF fingers with Al windows were adopted.
- Commissioning of the Halo Monitor at SACLA has been successfully carried out.

3. Things to do toward a versatile equipment,

- Improvement of lower/upper detection limit.
- Refinement of RF finger structure (reduce gap between a finger and a detector)
- Equipment with a cooling mechanism.